Princeton University
Department of Geology
Princeton, New Jersey

THEORETICAL CALCULATION OF THE SPECTRUM OF FIRST ARRIVALS IN LAYERED ELASTIC MEDIA

Robert A. Phinney

June, 1965

AFOSR Contract No.: AF 49(638) - 1243

Project Title: Research in Geophysics (Seismology)

ARPA order No.: 292-63, Amendment 7

ARPA project Code No.: 3810

Date Contract Starts: 1 July 1963

Date Contract Terminates: 30 June 1965

Amount of Contract: $96,429

Project Scientist Name and Telephone No.:
R. A. Phinney
452-4118

Princeton University
Department of Geology
Princeton, New Jersey

THEORETICAL CALCULATION OF THE SPECTRUM OF FIRST ARRIVALS IN LAYERED ELASTIC MEDIA

Robert A. Phinney

June, 1965

AFOSR Contract No.: AF 49(638) - 1243

Project Title: Research in Geophysics (Seismology)

ARPA order No.: 292-63, Amendment 7

ARPA project Code No.: 3810

Date Contract Starts: 1 July 1963

Date Contract Terminates: 30 June 1965

Amount of Contract: $96,429

Project Scientist Name and Telephone No.:
R. A. Phinney
452-4118

Abstract

A practical method for the calculation of the spectral parameters of first-arriving signals in seismology has been the object of much theoretical work in recent years. The difficulty has been in the fact that the first arrival usually behaves as an imperfectly trapped mode. Mathematically, it arises from the contributions of branch line integrals and complex poles. Attempts to transform the solution into a generalization of the normal modes have been a mathematical success only. Because of the complexity of this solution, a different, less elegant approach is demanded.

A practical technique is proposed. By a change of variable, the twice transformed solution is separated into a product of the form $f(u).e^{-iuR}$. This can be integrated with respect to the phase variable u, using standard quadrature methods, with the real part of u changing most rapidly along the integration path. By making the frequency complex, it is possible to displace any singularities away from the vicinity of the contour. This gives the spectrum of the signal as viewed through an exponentially decaying time window, making it possible to work with the first arrival by itself.

Introduction

The problem of an impulsive point source or line source in a layered elastic medium is central to the field of seismology. This is due as much to the fact that many earth problems can be modeled by a series of flat layers or spherical shells, as to the ease with which formal integral solutions can be written down. Basic methods are discussed by Ewing, Jardetzky, and Press [1957], and algorithms for treating the complete n-layered point source proble are presented by Harkrider [1964].

These solutions are useful only to the extent that they can be numerically evaluated. For example, the response to a line source (two-dimensional problem) has the form*

$$f(x,z,t) = \frac{1}{2\pi} \int_{-\infty}^{\infty} e^{i\omega t} \int_{0}^{\infty} \cos(kx) \, \frac{g(\omega,k,z)}{\Delta(\omega,k)} \, dk \, d\omega \qquad (1)$$

and the response to a point source (three-dimensional problem) has the form†

$$f(r,z,t) = \frac{1}{2\pi} \int_{-\infty}^{\infty} e^{i\omega t} \int_{0}^{\infty} k \, J_n(kr) \, \frac{g(\omega,k,z)}{\Delta(\omega,k)} \, dk \, d\omega \qquad (2)$$

The inner integrals

$$F(x,z,\omega) = \int_{0}^{\infty} \cos(kx) \, \frac{g}{\Delta} \, dk \qquad (3)$$

and

$$F(r,z,\omega) = \int_{0}^{\infty} k \, J_n(kr) \, \frac{g}{\Delta} \, dk \qquad (4)$$

give the Fourier transform of the impulse response. Since observed seismic signals may be readily transformed, evaluation of (3) or (4) may be considered an adequate numerical realization

*f is any observable such as a displacement or stress component

†n is usually 0 or 1, but may be larger for multipole sources. See Harkrider [1964].

of the theory.

Evaluation of the integral has always proceeded by some kind of transformation of the problem. Pekeris [1948] deformed the contour of integration in the complex k-plane in a way which separates the residue contributions due to real poles of the integrand (Fig. 1a and 1b). All singularities lie on the real k-axis if it is required that all radicals of the form $\nu = [k^2 - (\omega/v_n)^2]^{1/2}$ be taken with $Re(\nu) > 0$ on the sheet of integration. Branch points at $k = \omega/\alpha_n$ and $k = \omega/\beta_n$ constrain the transformed contour C' in Fig. 1b. All poles lie to the right of the branch points and to the left of the limiting point at $k = \omega/v_{min}$, where v_{min} is the least velocity in any layer. An ω-k diagram (Fig. 2) summarizes these relationships.

This transformation separates the solution into a sum of residue contributions and a branch line integral. The former, having phase velocities less than any halfspace velocity, are the trapped modes. Application of the stationary phase method gives the trapped modes as a function of time in a compact and physically meaningful form: the signal appears as a superposition of wave packets traveling with characteristic group velocities of the modes. This formalism is the basis for all work in surface wave kinematics, and has proved to be a satisfactory way to bring wave theory into seismological practice.

Description of the early-arriving signals from integrals (1) through (4) has proven more difficult. These events consist of the various refracted body phases which travel at high phase velocities-- i. e. the contribution from the branch line integral. Physically, the refraction arrivals may involve the same types of

resonance which produce the trapped modes, but the progressive loss of energy into the halfspace gives the so-called "leaking modes" instead. Mathematically, these resonances in the refraction arrival come about because complex poles lying on a Riemann sheet where $Re(\nu_n) < 0$ are sufficiently close to the branch line to affect the value of the branch line integral (Fig. 1b). Gilbert [1964], having investigated in detail the behavior of pole loci on the lower sheets, has suggested that his complex ω-k diagrams may be useful in connection with frequency/wavenumber analysis of data.

Recent work has concentrated on expressing the branch line integral in the same formalism which applies to the trapped modes (Rosenbaum [1960], Phinney [1961], Rosenbaum [1965]). This involves complicated transformations of the contour onto the lower Riemann sheets in such a way that the complex poles are "picked up" as residue contributions. Certain practical problems are involved in routinely calculating these leaking modes. In the first place, one is still left with line integrals which must be evaluated numerically; the fact that they represent only non-oscillatory signals does not eliminate their importance in the refraction problem. More bothersome is the problem of deciding which complex poles contribute to the signal; relevant poles must satisfy an "accessibility" condition in the complex $\omega(k)$ plane before a saddle point method may be applied. These problems, as well as the sheer magnitude of the mathematics, leave us, I think, with a method which can never be used routinely for problems in earth structure by other than a dedicated specialist.

Direct Evaluation of the Integrals on a Computer:

In this paper my object is to investigate the possibility of numerically evaluating integrals such as (1) - (4) on a digital computer. For the sake of discussion, I will concentrate on (3), the Fourier transform of the line source seismogram. Fortunately, the elegance of contour integration is still at our disposal, making it possible to consider several ays to go about the integration.

A minimum requirement is that the integrand must vary smoothly enough along the contour to permit approximation of the integral by a sum. When x is large, this may be troublesome, owing to the cos(kx) factor. A method due to Filon [1928] avoids this problem by taking account of the cosine function in formation of each of the contributions to the sum. Essentially a generalization of Simpson's rule, the Filon method requires only that g/Δ vary slowly within the interval of approximation. By considering only cases for which both source and receiver are near or within the layered part of the structure, we have only to worry about the behavior of g/Δ in the neighborhood of the contour of integration (the restriction on source and receiver will be removed later).

Evidently the contour pictured in Figure 1a is unsatisfactory by this standard, since it passes over all the singularities. The obvious solution is to transform to C' in Figure 1b, and remove the trapped mode poles from the problem, leaving a fairly well-behaved branch line integral. While this may be satisfactory for many values of ω, it leads to difficulty when the integral must be evaluated for a series of closely spaced frequencies

(for this is what constitutes a spectrum). In the neighborhood of each cutoff frequency, a normal mode pole passes through the branch point from the lower to the upper Riemann sheet (Fig. 2). Then g/Δ varies too rapidly near the branch point for a numerical method to be usable. Furthermore, if this pole is to the right of, but very close to the branch point, its effect will have already been subtracted out as a residue contribution, and we will be in the position of adding in a nearly equal contribution of opposite sign. It is not possible to ignore these cutoff frequencies, since they provide the most important contributions to the refraction arrival. Further manipulation of C' would lead to transformations on the lower sheet like those which have already proven to be too cumbersome.

We are led back to consideration of the situation in Fig. 1a. Two apparent ways to smooth the integrand along the contour are (Fig. 3a and 3b): a) deform the contour upward in the k-plane to avoid the singularities and b) move the singularities into the fourth quadrant. It is important to note that the second of these methods changes the problem itself, since an analytic function is determined by its singularities. This is done by making ω a complex variable $\bar{\omega} = \omega - i\lambda$; the singularities then lie along a straight line in the fourth quadrant which passes through the origin. An investigation of how (b) changes the problem will show that only the modified problem is at all reasonable and why, as a consequence, method (a) must fail.

Consider the Fourier pair relating a signal f(t) and its transform $F(\bar{\omega})$, where the bar over ω denotes that ω is considered as a complex variable $\bar{\omega} = \omega - i\lambda$:

$$f(t) = \frac{1}{\sqrt{2\pi}} \int_{-\infty}^{\infty} e^{i\bar{\omega}t} F(\bar{\omega})\, d\bar{\omega} \tag{5}$$

$$F(\bar{\omega}) = \frac{1}{\sqrt{2\pi}} \int_{-\infty}^{\infty} e^{-i\bar{\omega}t}\, f(t)\, dt \tag{6}$$

If $f(t)$ is identically zero prior to $t = 0$, then F is analytic in the lower half plane, and the path of integration in (5) may be run along the line $Im(\omega) = -\lambda$ = constant. The functional values of F along this path are precisely the same function implied if we evaluate (3) for complex ω, since we have performed analytic continuation of functions identical on the real axis $\lambda = 0$. Calling this modified transform F_λ, we then get, by a trivial change of variable:

$$[e^{-\lambda t}\, f(t)] = \frac{1}{\sqrt{2\pi}} \int_{-\infty}^{\infty} e^{i\omega t}\, F_\lambda(\omega)\, d\omega \tag{7}$$

$$F_\lambda(\omega) = \frac{1}{\sqrt{2\pi}} \int_{-\infty}^{\infty} e^{-i\omega t} [e^{-\lambda t}\, f(t)]\, dt \tag{8}$$

Thus the modified transform is a function obtained by premultiplying the data $f(t)$ by $e^{-\lambda t}$ and Fourier transforming in the usual way. We have, in effect, smoothed the spectrum. It is significant that this comes about in an attempt to find a practical way to do an integral; in retrospect, it will be apparent that an unsmoothed spectrum will be an exceedingly ill-behaved function of frequency which is difficult to represent by a table of values produced by a computer.

The impulse response of a simple layered system persists to times greatly in excess of the slowest direct body wave arrival time, due to the partial trapping of energy bouncing at near vertical angles in the waveguide. A faithful representation of the Fourier transform requires that a very long time interval be

analyzed; in the absence of smoothing, this spectrum can vary sharply within frequency intervals equal to the reciprocal of the time interval. Matters become most serious in the rapid variation of the phase with frequency, which leads, in the case of a computer-produced table, to ambiguity in the total phase angle. Anyone who has computed "accurate" Fourier spectra from short-period vertical signals can especially appreciate the problems involved.

The result is that, if numerical results are an objective, and one must deal with discrete valued functions computed at discrete frequency spacings, the "true" unsmoothed spectrum is worthless†. It is too sensitive to small errors and to details of the analysis. In fact, the most natural way to smooth is to premultiply the signal by a damped exponential, since the theoretical problem can be solved by evaluating (3) at complex ω. The alternative method, shown in Fig. 3a, is unacceptable, since the result must be the unsmoothed spectrum; one would find that amplification of the singularities by an exponential in the imaginary part of k would cancel out any smoothing of the integrand obtained by moving away from the singularities.

It can now be said that we have a wave theory for first arrivals. How "first" an arrival we are talking about lies in the arbitrary character of λ. An intelligent decision requires understanding of the problems of a particular application, and will depend on such parameters as distance, source spectrum, and the amount of detail desired. In an application with little

† A possible exception would be an expecially "leaky" waveguide with a very short response time, such as a high velocity layer on a low velocity substratum.

advance knowledge about the unknown earth structure, one wants to use a large λ, to provide strong smoothing and a relatively small number of degrees of freedom in the data. When data and theory can be reconciled at this level, another approximation to the correct structure may be studied by working with a longer time window (smaller λ). While it may be premature to mention this, a very desirable feature of this approach is that the inversion problem for body wave spectrums seems to have a natural solution in terms of this sequence of smaller and smaller λ.

A salient property of the solution is that it is a single function which contains spectral information bearing in some degree (depending on λ) on all portions of the signal. All trapped modes as well as all leaking modes and undispersed body phases are described; only by a choice of λ can the relative contribution of the later-arrivals be made small. This is of course a limitation in working with the better understood well-dispersed surface waves, for which group and phase velocity are very useful concepts. In multilayered systems, however, the higher modes often have a complicated group velocity behavior by which they add up into the body wave arrivals from intermediate layers. Such a mode sum is more conveniently looked at directly, through its smoothed spectrum.

Further Practical Matters:

We have shown that numerical difficulties associated with evaluation of the line source solution (3) can be avoided by combining Filon's method with use of a complex frequency. Before looking at examples, it is necessary to cover some matters of technique.

1. Truncating the infinite integral: It is impractical to evaluate the contour integral for large enough values of k to reduce the truncation error to an acceptable (1%) level. The entire half-plane to the right of the last singularity is analytic, allowing (3) to be split into positive and negative exponentials:

$$F_{\lambda}(x,z,\omega) = .5\int_{-\infty}^{\infty} e^{ikx}(g/\Delta)\,dk \quad + \quad .5\int_{-\infty}^{\infty} e^{-ikx}(g/\Delta)\,dk \tag{9}$$

and the respective contours to be deformed into the upper and lower half planes as shown in figure 4, with the turning point beyond the last singularity. These two line integrals converge rapidly, and can be evaluated by any of the standard quadrature methods.

2. The high frequency problem: For a fixed choice of λ a computed spectrum becomes more and more complicated as higher frequencies are considered. This is due to the interaction of many "modes", producing beats in the spectrum. When going to higher frequencies with a fixed time window, one is getting a larger number of degrees of freedom associated with the large number of cycles in the analysis interval. In a program aimed at data analysis and interpretation, there is no reason why λ cannot be increased in proportion to ω, giving a time window

which is variable, but in fixed proportion to the period being analyzed. The spectrum will then have the same number of degrees of freedom per frequency interval at all frequencies; ω may be considered as varying along the contour OA in figure 5. The constant λ case is contour BC. To differentiate them from the raw, unsmoothed spectrum let BC define the λ-spectrum and path OA the ψ-spectrum, since the latter preserves the phase angle ψ of ω. Subsequent discussion about the λ-spectrum will refer to the ψ-spectrum unless exception is made.

An obvious extension of these notions is to evaluate the spectrum on the contour OD or EF. These are, respectively, the Laplace transform of the signal or the Laplace transform of the signal as premultiplied by $e^{i\omega t}$. Complete knowledge of either of these implies complete knowledge of the spectrum on any other contour, such as OA or BC, since F is analytic in the lower half plane, and we may go from one contour to another by analytic continuation. The difficulty is that analytic continuation cannot be performed with numerical data on a contour, since we do not know all the derivatives of F on that contour. This is exactly the same as attempting to solve an elliptic differential equation by applying numerical operators to the data on an initial value line; the problem is said to be ill-posed. The same may be said of attempting to perform an upward continuation of data on OA or BC; then, however, we have a reasonable amount of information in our data and do not want continuation. In contrast, the Laplace spectrum is virtually devoid of information which can be seen above the numerical noise. The situation is illustrated in Fig. 6, which shows a Laplace spectrum and

a λ-spectrum.

3. Extension to the point source problem: The essence of Filon's method is that the integral is divided into subintegrals of the form

$$\int_{k_i-\delta}^{k_i+\delta} \cos(kx)(g/\Delta)\, dk \qquad ;$$

if g/Δ varies slowly enough, it can be represented by a second degree polynomial in the interval. Knowing the indefinite integral $\int\cos(kx)[a+bk+ck^2]dk$, we can then write down a quadrature formula, with δ a parameter. The equivalent operations for the point source reduce to the problem of knowing the indefinite integral

$$I(k_i,\delta,n,p) = \int_{k_i-\delta}^{k_i+\delta} J_n(kr)(k-k_i)^p dk$$

Term by term integration of the power series for the integrand gives a power series for the integral in terms of δ and k_i. By application of the theory of Taylor series, this power series can be re-expressed as an expansion about some new point k_o, giving a rapidly converging series in δ and (k_i-k_o). As far as numerical objectives are concerned, this integral may be regarded as a known function, which can be generated on a computer as readily as the trigonometric functions. For values of k_i larger than about 15, it is desirable to have an asymptotic formula for the integral. Manipulations leading to such a formula are straightforward and will not be discussed here. We can conclude that the point source solution requires a little more programming than the line source, but does not differ in any substantive way.

4. Extension of the line source problem to admit a source in the halfspace: This is best handled by an illustrative case. If we assume a line source and receiver both located in the

halfspace (figure 7), then the response has the form

$$F_\lambda = \int_{-\infty}^{\infty} e^{-i(kx + \nu'_{\alpha 2} Z)} q(\omega,k)\, dk \tag{12}$$

where $\nu'_{\alpha_2} = \sqrt{K^2 - k^2}$; $K = \omega/\alpha_2$; $Z = z + h$.

We want to put this in the form

$$F_\lambda = \int e^{-iuR} q(\omega,k(u)) \frac{dk}{du}\, du \tag{13}$$

and integrate along a path such that either Im(u) = constant or Re(u) = constant. The methods described earlier in this paper will then be applicable.

Set $x = R \cos\theta$ $\qquad k = K \cos\eta$

$Z = R \sin\theta$ $\qquad \nu'_{\alpha 2} = K \sin\eta$

Then $\quad kx + \nu'_{\alpha 2} Z = KR\cos(\eta - \theta)$

or $\quad u = K\cos(\eta - \theta) = k\cos\theta + \nu'_{\alpha 2}\sin\theta \qquad (14)$

We can solve for k(u) in this special case:

$$k = u\cos\theta + \sqrt{K^2 - u^2}\,\sin\theta \tag{15}$$

with $$\frac{dk}{du} = \cos\theta - \left(\frac{u}{\sqrt{K^2-u^2}}\right)\sin\theta \tag{16}$$

We are in a position to make use of (13). The mapping of the real k-axis onto the u-plane is described by (14) and shown in figures 8a and 8b. Point A, at $u = K\sin\theta$, is the map of $k = 0$; for small k, u is real and increasing, as can be seen from the derivative

$$\frac{du}{dk} = \cos\theta - \left(\frac{k}{\sqrt{K^2-k^2}}\right)\sin\theta$$

which vanishes at $k = K \cos\theta$, the well known stationary phase point, where $\theta = \eta$. Point S, at $u = K$, is the map of this stationary phase point, and represents a singularity where the mapped contour reverses direction. This singularity (an additional branch point in the u-plane) will provide an important part of the value of the integral. Point B, at $k = K$, $u = K \cos\theta$, is the singularity where du/dk is undefined, and the contour moves into the complex u-plane. The ambiguity in the square root is resolved by the original condition that $\mathrm{Re}(\nu_{\alpha 2}) > 0$, which, in light of $\nu_{\alpha 2} = i\nu'_{\alpha 2}$, requires that $\mathrm{Im}(\nu'_{\alpha 2}) < 0$. The remainder of the contour is a limb of a hyperbola in the fourth quadrant, asymptotic to the line $-\mathrm{Im}(u)/\mathrm{Re}(u) = \tan\theta$. The remaining singularities of the integrand are folded into the interval ASB on the real axis.

For reasons discussed earlier, the frequency must be taken with a negative imaginary part. The mapping of the real k-axis is shown in figure 8b. The points A, B, and S have moved into the fourth quadrant, but are defined as in the previous paragraph. All other singularities lie on the line segment ASB. The contour AC is the image of the real k-axis. AC can be deformed into the path AHJ without crossing any singularities; the integration from A to H is done by Filon's method and the rapidly converging integral from H to J by any common quadrature formula. This final transformation demonstrates an important physical result-- that the predominant contributions to the integral come from the singularities between A and S, including the stationary phase contribution itself. Singularities lying on the (folded) segment SB will not contribute significantly. In the original variables,

this means that wave numbers greater than the stationary phase value do not contribute, or that phase velocities less than the critical phase velocity do not contribute.

To carry out the integration it is necessary to know the complex values of k corresponding to points on the contour AHJ. For the problem just described, a solution (15) can be written down. A more general case is the partial ray integral

$$F_\lambda = \int_{\infty}^{\infty} e^{-i(kx + \nu'_{\alpha 2}h + \nu'_{\beta 2}z)} q(\omega,k)\, dk \tag{17}$$

which describes an upgoing P-wave coupled to the layer, coupled in turn to a downgoing S-wave. The defining equation for the phase function u becomes

$$uR = kx + \nu'_{\alpha_2}h + \nu'_{\beta 2}z \tag{18}$$

where R is some characteristic distance which we would normally take as the optical distance for the PS reflection. Inversion to give k as a function of u must be done numerically, since (18) cannot be solved algebraically. With a slight change in notation, (18) is the same equation which must be solved to get the Cagniard-deHoop path used in the Cagniard method. None of the further elegance of this technique is of use in boundary value problems involving more than one interface.

5. Combining the previous two problems-- a point source in the halfspace: The method must embody features from the preceding two sections; no attempt is made in this paper to do the problem.

Later arrivals, filtering, and the refraction problem:

The numerical λ-spectrum described here most naturally is applied to the first arrival-- invariably some sort of P-wave. It is of practical interest to study the extent to which one can look at later-arriving body waves.

1. Partial ray expansions: $\Delta(\omega,k)$ contains sums of exponentials in the various layer parameters. Various binomial expansions of g/Δ may be formed, each corresponding to a particular way of partially decomposing the solution into rays. An example of one term in such an expansion is (17), where we can identify exponential phase factors describing ray propagation and a generalized reflection coefficient giving the complete response of the layers involved. Many of the later-arriving body phases can be established as first-arrivals of a partial ray integral. One must be reasonably sure, when looking at data, however, that the body phase being studied is not contaminated by earlier-arriving energy. Somewhat more limiting is the fact that each partial ray gives rise to more than one refraction arrival in addition to the principal optical ray event. These refractions cannot be separated by further decomposition of the integrand. The situation is illustrated in figure 9. The partial ray is defined by the geometrical path PS (and has the same form as in (17)). Evaluation of the integral and formation of the impulse response would give a seismogram containing:

a) the first arrival, a refracted event PpS

b) a refracted event PsS

c) the reflection PS

No manipulation of partial rays can separate these three events.

In addition, the refraction PpP arises from a different partial ray entirely, but may arrive so close to PpS that separation of the phases is not possible. It would be necessary in this case to compute at least these two partial rays.

2. Filtering in the ω-k plane: From our understanding of the kinematics of propagation of body phases, we may discriminate against the first arrival on the basis of its phase velocity, in effect transforming a later arrival into the first arrival. Since filtering can be done by simple multiplication in the variables ω and k, multiplication of the integrand by a velocity filter can be used to reject higher phase velocities associated with first arrivals. Normal care in the design of the filter is still required; a conservative procedure would be to use only filters with physical analogs in simple array processing.

3. Windowing by convolution: It has been shown that use of the complex frequency variable provides the effect of an exponential window in the time domain. It would be desirable to have more general windows available, such as a lagged exponential, which could be used to select later-arriving body waves. I can see no other way of doing this except directly-- by applying a convolution operation in the frequency domain. This adds another integration, which would be as much work as computing the impulse response directly by Fourier synthesis.

4. Crossover of refraction lines from different layers: An obvious application of the λ-spectrum is to first arrivals at intermediate refraction distances where two or more refraction lines have nearly identical arrival times. When a refraction, such as line 2 in figure 9, does not appear as a first arrival,

its identification from later arrivals at large distances can be a serious problem. Even if it appears as a first arrival in a short distance interval, the distribution of geophones may be such that it can only be seen at one station, in which case the slope, or even the identification of the line is in doubt.

Since the λ-spectrum contains all the information inherent in the wave solution for the time window and frequency band under consideration, it is appropriate to work with it at several distances near the crossover. The result is an extended type of refraction plot: a λ-spectrum versus distance, which constitutes a surface or a nest of curves. It would be the object of the refraction study to adjust the model parameters to bring the theoretical and experimental spectrum-distance data into agreement.

This is one of a class of problems in which geometrical optics gives more than one arrival line with nearly the same travel time. The neighborhood of a cusp in a travel time curve is of this nature. The multiple branches of the PKP phase which grazes the inner core are an example in a spherical geometry. To interpret the data in terms of ray theory, one must be able to distinguish separate arrivals, no matter now close they are in time, and to identify the point of a cusp. Neither is possible with seismic data recorded on an instrument with a finite passband. In practice, conventional short period seismometers come close enough in the PKP example to show the existence of several branches; it cannot be shown, however, whether other branches have been missed, or whether the identification of the cusps is correct. This latter problem comes about because of the existence of a diffracted pulse at stations in the geometrical shadow.

The principle of a λ-spectrum-distance profile can be used to resolve problems of this nature. It will be possible to use conventional long-period seismometers for wave theory interpretations of earth structure at certain depths where diffraction effects are important: the base of the upper mantle at 400+ km; the core-mantle boundary; the inner core boundary. This paper does not describe any calculations of the spectrum in a spherical geometry. There are, however, no real obstacles to doing so.

Calculation of phase velocity, attenuation, and group velocity:

Phase velocity and attenuation are basic notions in the kinematics of traveling waves, and are easily applied in a description of trapped modes. When studying arbitrary transients containing various types of waves, these variables must be regarded merely as derived quantities, defined by certain operations with the λ-spectrum of the signal.

Writing the spectrum $F_\lambda = A\, e^{i\phi}$ (19)

we define the phase velocity c, by

$$c = \frac{\omega}{\left[\frac{\partial\phi}{\partial x}\right]} \tag{20}$$

and the attenuation coefficient, γ by

$$\gamma = -\frac{1}{A}\frac{\partial A}{\partial x} \tag{21}$$

By differentiation of (19):

$$\frac{\partial F_\lambda}{\partial x} = \frac{\partial A}{\partial x} e^{i\phi} + A i \frac{\partial \phi}{\partial x} e^{i\phi} \tag{22}$$

and division by (19):

$$\frac{1}{F_\lambda}\frac{\partial F_\lambda}{\partial x} = \frac{1}{A}\frac{\partial A}{\partial x} + i\frac{\partial\phi}{\partial x} \tag{23}$$

we get:

$$c = \frac{\omega}{\mathrm{Im}\left(\frac{1}{F_\lambda}\frac{\partial F}{\partial x}\right)} \tag{24}$$

and:

$$\gamma = -\mathrm{Re}\left(\frac{1}{F_\lambda}\frac{\partial F}{\partial x}\right) \tag{25}$$

To form $\frac{\partial F_\lambda}{\partial x}$ from the theoretical solution, differentiate (3):

$$\frac{\partial F_\lambda}{\partial x} = -\int_0^\infty k \sin(kx)\,(g/\Delta)\, dk \tag{26}$$

From (26) we can compute $\frac{\partial F_\lambda}{\partial x}$ by Filon's method at the same time that we compute F_λ. The theoretical phase velocity and attenuation follow from (24) and (25). It will become apparent from the numerical examples to follow that these functions are not always very diagnostic when several modes or rays contribute to the λ-spectrum.

The taking of a derivative by means of an analytic relation such as (26) does not eliminate the amplification of error which occurs in the derivative operation. It is found that, in general, calculations of c and γ have about one less decimal place of accuracy than do the calculations of F_λ itself.

A derived group velocity, U, can be defined by

$$U = \frac{x}{t} = -\frac{x}{\frac{\partial \phi}{\partial \omega}} \tag{27}$$

This is based on the fact that the impulse response integral

$$f(t) = \int A(\omega)\, e^{i(\omega t + \phi)} d\omega \tag{28}$$

receives its greates contribution at time t from the frequency for which $\frac{\partial}{\partial \omega}(\omega t + \phi) = 0$. Equation (27) follows. Like phase velocity, U is of limited usefulness in looking at an arbitrary transient. Further difficulty lies in the necessity of either programming the analytic form of $\frac{\partial \phi}{\partial \omega}$ or obtaining the derivative by simple differencing. An illustrative example will use the latter method.

Numerical examples:

Calculations are shown for the line source response for the liquid layer/liquid halfspace and liquid layer/solid halfspace problems. Parameters are listed in Table 1.

Model	α_2	β_2	ρ_2
LPLTE1	-	-	-
LOL002	3.0	-	2.5
LOS002	3.0	1.732	2.5
LOS010	3.0	.95	2.5
LOS011	3.0	.40	2.5
LOS012	3.0	.70	2.5
LOS013	3.0	1.30	2.5

Table 1. Layered models used for calculations. For all models $H_1 = 1.0$, $\alpha_1 = 1.0$, $\rho_1 = 1.0$, for normalization.

Expressions for g/Δ are in Ewing, Jardetzky, and Press [1957], chapter 4.

Model LPLTE1 is unique in having a residue series solution which is complete, and which is unencumbered by a branch line integral. To provide a check of the numerical integration program, the spectrum for this model was obtained in two different ways: first by substituting $\rho_2 = 0$ in the liquid/liquid kernel g/Δ, and then by using the residue series.

If an acceptable numerical noise level is 1 or 2 in the third decimal, then it is found that $\Delta k = .04$ is a small enough spacing provided that $\lambda \geq .15$ and $x \leq 20$. On the IBM 7094, calculation of 100 spectral values takes about 5 minutes for the liquid/liquid problem and about 7 minutes for the liquid/solid problem. When computing a λ-spectrum for a set of different x, however, the same values of g/Δ are generated in each pass. By saving these

values in a high speed backup storage (disk file) and reusing them in the second and succeeding passes, the time requirement is reduced to about 40 seconds per case for all but the first.

While the limitation to $\lambda \geq .15$ is not serious, the restriction that x not be too large is annoying. This comes about from accumulation of roundoff error in forming the sum of contributions from the various k-intervals. As x increases, one is adding up the same table of g/Δ values with different weights; for larger x, the values tend to cancel, and roundoff becomes a problem. To a limited extent, this can be overcome by grouping terms or by selecting $x\Delta k$ to be a multiple of 2π and grouping. A more satisfactory resolution of the problem is deferred at this time.

The notion of a profile of λ-spectrum versus distance is illustrated in figure 11, which shows model LOL002, with $\lambda = .15$, $h = 1.3$, and $z = 0.1$. For a liquid/liquid case, the early arriving signal is very nearly described as a sum of dispersed normal modes (Pekeris [1948]), with the branch line integral contributing a relatively weak signal. Our curves should reflect, therefore, the mode character of the response. Most of the energy is concentrated around the theoretical cutoff frequencies of the first two modes at .26 and .78, due to the source being in the halfspace. The irregular behavior (for x = 7 and 10) at the higher frequencies is due to the effect of mode mixing.

Figure 12 gives phase velocities and a single instance of group velocity for this model. The mode-like character of the signal is demonstrated by the invariance of c with x. The effect of the branch line integral is automatically included at frequencies near cutoff, causing c and U to behave differently from c

given by mode theory. The variability of c in the vicinity of the second mode cutoff (due to mode interference) demonstrates the kind of limited service that can be expected of this parameter at higher frequencies.

A comparable example for the liquid/solid problem LOS002 appears in figure 13. The irregular structure of the amplitude function is a result of mixing the first-arriving PL mode with the trapped modes. Even though $\lambda = .3$ in this case, giving a shorter time window, the trapped modes still arrive in the time covered by the window except at the greatest distances.

The effect of the basement shear velocity at a given distance is shown by figure 14. In all other respects, this analysis has the same parameters as the liquid/liquid case in figure 12. By letting β_2 become small we have a check on the liquid/solid calculation. When it is as small as 0.4, the agreement with the liquid/liquid result is good; for values greater than 1.0, the spectrum is mainly determined by the existence of the trapped shear modes. At the lower shear velocities, the shear and surface wave energy arrives so late that it is excluded by the exponential time window, and we see only the effect of the P modes. The phase velocity (figure 15), being a derivative quantity, is rather ill-behaved by comparison with the spectrum itself, and the agreement with the liquid/liquid case is achieved only at the lowest values of β_2. Discontinuities in c appear near minima in the amplitude spectrum.

My viewpoint in this paper has been that the λ-spectrum is an appropriate function to work with in data analysis. The preceding examples demonstrate that its behavior may be sufficiently

strange to most workers that a demonstration is in order. The λ-spectrum has been computed for LOS002 at x = 20. for an increasing sequence of λ (figure 16). Fourier synthesis has been applied to each spectrum to yield a theoretical seismogram-- as modified by the exponential window. To reduce the effect of chopping the λ-spectrum at a particular frequency, a realizable low-pass filter has been applied before synthesis. The results appear in figure 17. The creation of a theoretical seismogram appears to be the only process in which the λ-spectrum is preferable to the ψ-spectrum (which has the virtue of smoothness at high frequency). If Fourier synthesis is based on a ψ-spectrum, the theoretical time function is a peculiar modification of the full seismogram, in which each frequency has been premultiplied by a different time window. This time function would appear as though it had been generated by a set of constant-Q delay lines, in which the attenuation coefficient is proportional to frequency.

Conclusion:

It has been shown that the requirement of numerically realizing the theoretical response of a layered medium leads naturally to the conclusion that signals must be viewed through a decaying exponential time window. The ultimate object of such work is to be able to use comparisons between theory and data to determine velocities and densities in the earth. At the present time, however, data processing technique is considerably more advanced than the theoretical work, and a considerable amount of computer programming must be done to close the gap. This includes not only complete realizations of the methods described in the text (or alternate methods), but a realization of available formal schemes for obtaining the response function in multilayered media. From a practical point of view, the Thomson-Haskell matrix method should be supplemented or replaced by methods based on a continuous velocity-depth function which will be faster by virtue of their dependence on fewer independent parameters. For example, the base computing time for one spectrum is 5 minutes in the most elementary case: if 20 solid layers were required to model an earth structure, the time could go over 200 minutes per curve--for the same amount of output information. A compensating factor will be the availability in the near future of computers which can provide 10-100 times the computing speed of present models.

Despite this present lack of theoretical capability to match with data analyses, it is clear that work in data processing of body waves must be affected by the importance of the exponential window. Demonstrations must be made of the way in which the

λ-spectrum varies with distance and choice of smoothing parameter. In cases where the source is controlled or sufficiently known, it is necessary to establish the repeatibility of the result over a given path, and to determine the relation between λ and the repeatibility. In the area of data analysis techniques, it does not appear that work with sets of analysis functions more sophisticated than the damped exponentials can be meaningfully related to wave propagation theory . This comes back to the elementary fact that the complex exponentials are the correct choice of functions for separation of the wave equation.

Acknowledgments

This research was supported by the Air Force Office of Scientific Research under contract AF 49(638)-1243 as a part of the Advanced Research Projects Agency's Vela-Uniform Program. Use was made of computer facilities supported in part by National Science Foundation grant NSF-GP579.

References

Ewing, M., W. Jardetzky, and F. Press, Elastic Waves in Layered Media, McGraw-Hill, 1957.

Filon, L. N. G., On a Quadrature Formula for Trigonometric Integrals, Proc. Roy. Soc. Edin., XLIX, 38-47, 1928-29.

Gilbert, F., Propagation of Transient Leaking Modes in a Stratified Elastic Waveguide, Rev. Geoph., 2, #1, 123-154, Feb. 1964.

Harkrider, D. G., Surface Waves in Multilayered Elastic Media 1. Rayleigh and Love Waves from Buried Sources in a Multilayered Elastic Half-space, Bull. Seis. Soc. Am., 54, #2, 627-680, April 1964.

Pekeris, C. L., Theory of Propagation of Explosive Sound in Shallow Water, Geol. Soc. Amer. Memoir 27, 1948.

Phinney, R., Leaking Modes in the Crustal Waveguide. Part 1. The Oceanic PL Wave., Jour. Geophys. Res. 66, #5, 1445-1470, May 1961.

Rosenbaum, J., The Long-Time Response of a Layered Elastic Medium to Explosive Sound, Jour. Geophys. Res., 65, #5, 1577-1613, May 1960.

Rosenbaum, J., Transmission of Explosive Sound Through a Fluid Layer over an Infinitely Deep Elastic Bottom, unpublished manuscript.

Appendix

1. Conventional geometry of a layered system:

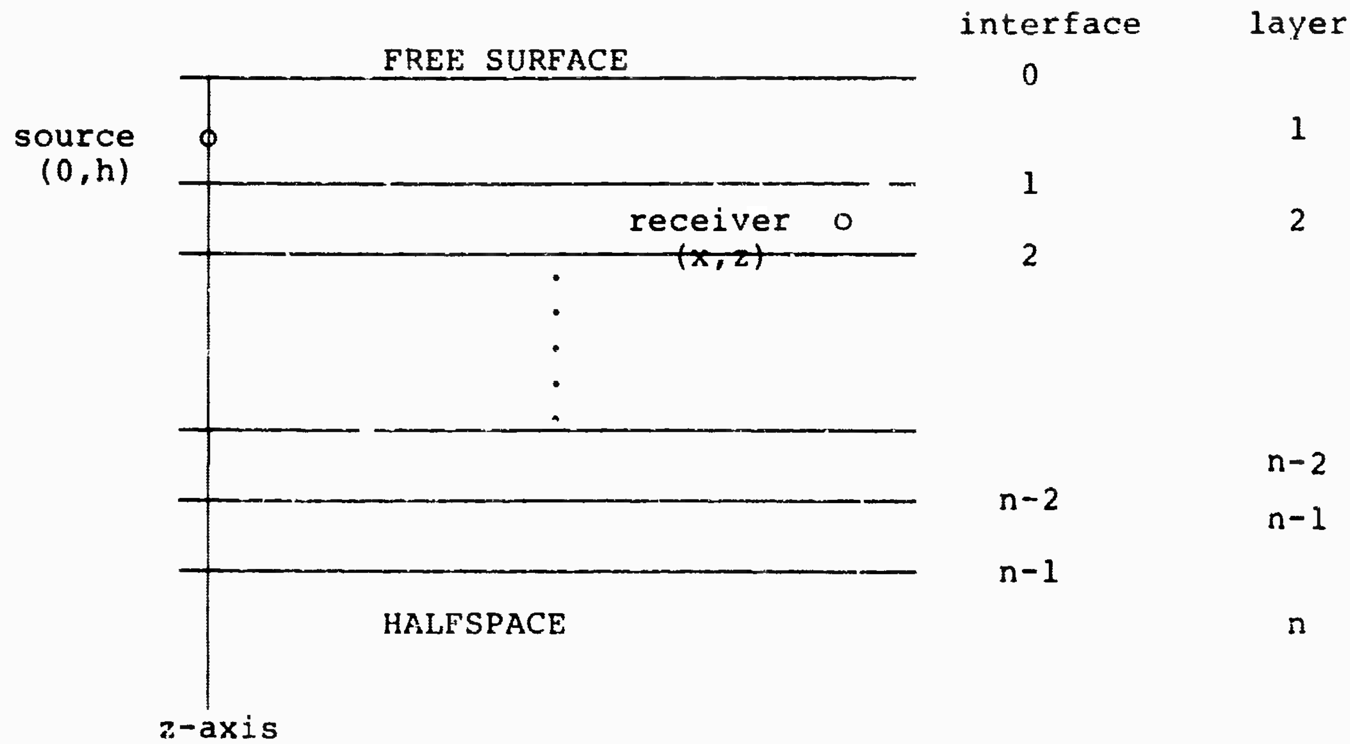

2. Notation:

A	amplitude of the spectrum
c	phase velocity
f	some field variable in the time domain
F	some field variable in the frequency domain
h	depth of source
H_i	thickness of ith layer
k	horizontal wave number
n	used as a subscript referring to the halfspace
r	radial coordinate of receiver in cylindrical coordinates
t	time
u	phase variable (equation 14)
U	group velocity
v	denotes a body velocity, either α or β
x	horizontal distance from source to receiver (line source problem)

2. Notation (continued):

α_i	compressional velocity in ith layer
β_i	shear velocity in ith layer
γ	attenuation coefficient
θ	ray angle (equations 13-14)
η	wave angle (equations 13-14)
λ	(negative) imaginary part of complex frequency
$\nu_{\alpha i}$	$\sqrt{k^2-(\omega/\alpha_i)^2} \quad = i\nu'_{\alpha i}$
$\nu_{\beta i}$	$\sqrt{k^2-(\omega/\beta_i)^2} \quad = i\nu'_{\beta i}$
ρ_i	density in ith layer
ϕ	phase angle of spectrum
ψ	minus phase angle of $\bar{\omega}$
ω	angular frequency
$\bar{\omega}$	complex frequency variable = $\omega - i\lambda$

3. Filon's method:

This is a method of numerically integrating trigonometric integrals of the form

$$I = \int_a^b \cos(xp)\ f(p)\ dp$$

where x may be large. Let the range be divided into 2n equal parts with an interval h such that

$$b = a + 2nh$$

After representing f(p) over the interval $[a+(s-1)h\ ,\ a+(s+1)h]$ by a second degree polynomial whose coefficients can be determined, we get, after some manipulation

$$I = h[\alpha\{f(b)\sin(xb) - f(a)\sin(xa)\} + \beta C_{2s} + \gamma C_{2s-1}]$$

where, if $\theta = xh$,

$$\alpha = \theta^{-3}\{\theta^2 + \theta\sin\theta\ \cos\theta - 2\sin^2\theta\}$$

$$\beta = \theta^{-3}\{\theta[1 + \cos^2\theta] - 2 \sin\theta \cos\theta\}$$

$$\gamma = 4 \theta^{-3}\{ \sin\theta - \theta \cos\theta\}$$

and

$$C_{2s} = \sum_{j=0}^{n} f(a+2jh).\cos[x(a+2jh)] - \frac{1}{2}[f(b)\cos(bh)+f(a)\cos(ah)]$$

$$C_{2s-1} = \sum_{j=1}^{n} f[a+(2j-1)h].\cos\{x[a+(2j-1)h]\}$$

A complete description of the method is given by Tranter [1956], following the original paper by Filon [1928].

Figure Captions

1a. k-plane for integration of (3), and initial contour, showing singularities on the real axis.

1b. k-plane for integration of (3), with the contour deformed into path C' around the branch cut.

2. ω-k diagram for singularities of the integrand on the top sheet.

3a. Numerical integration by deforming the contour away from the singularities.

3b. Numerical integration by moving the singularities into the fourth quadrant.

4. Truncation of the integral by splitting into exponentials and deforming the respective contours into the upper and lower half-planes respectively.

5. ω-plane. Examples of lines along which the spectrum may be computed.

6. Comparison of computed Laplace and λ-spectrum for model LOS002. Curves are separately normalized.

7. Geometry for a source and receiver in the halfspace.

8a. u-plane, showing map of the real k-axis, using (14), when ω is real.

8b. u-plane, showing map of the real k-axis, using (14), when $Im(\omega)$ is negative. The deformed contour AHJ is used in the numerical evaluation of (13).

9. Geometry for a PS partial ray integral in a three-layer model.

10. Illustrative travel-time curve for a three-layer model with a masked refraction arrival.

11. Model LOL002: λ-spectrum as a function of distance for $h= 1.3$, $z= 0.1$, $\lambda= .15$, due to an impulsive line pressure source.

12. Model LOL002: Phase velocity spectrum as a function of distance and a single example of group velocity, obtained from the λ-spectrum of Figure 11.

13. Model LOS002: λ-spectrum as a function of distance for $h= 0.9$, $z= 0.1$, $\lambda= .30$, due to an impulsive line pressure source.

14. Dependence of λ-spectrum on β_2, for a sequence of models with decreasing shear velocity in the halfspace, at x= 10., h= 1.3, z= 0.1, λ= .15. The limiting case of β_2= 0 is computed using a liquid/liquid program.

15. Phase velocity spectrum for the models computed in Figure 14.

16. Model LOS002: λ-spectrum as a function of λ for x= 20., h= 1.3, z= 0.1 due to an impulsive line pressure source.

17. Model LOS0[illegible] : Impulse response obtained by Fourier synthesis of spectrum in Figure 16.

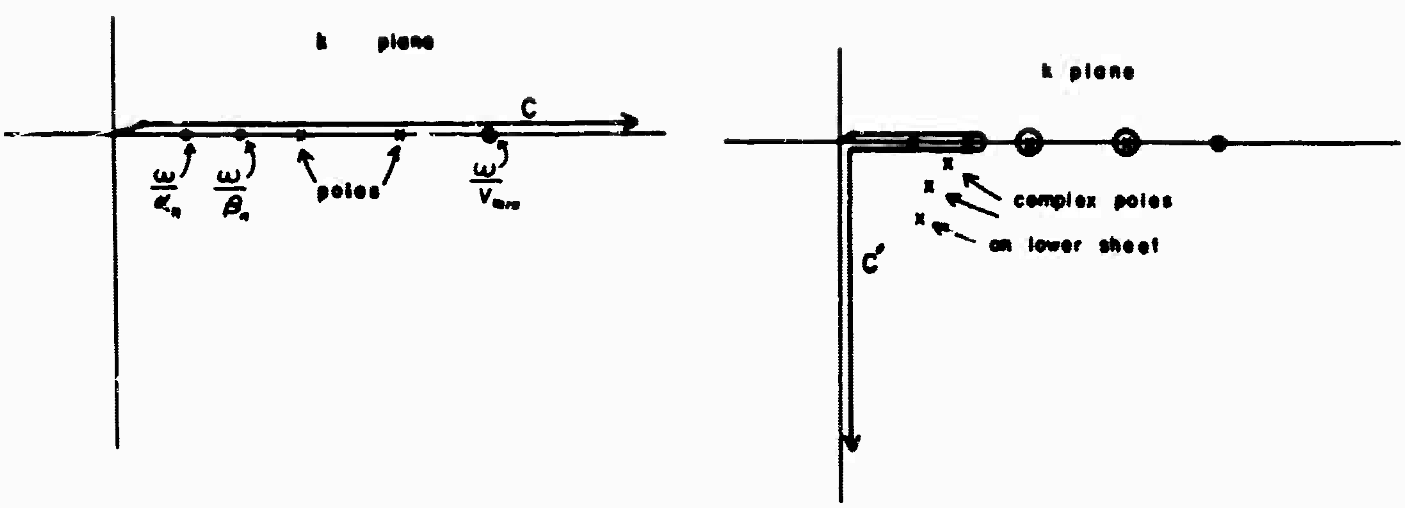

Figures 1a and 1b

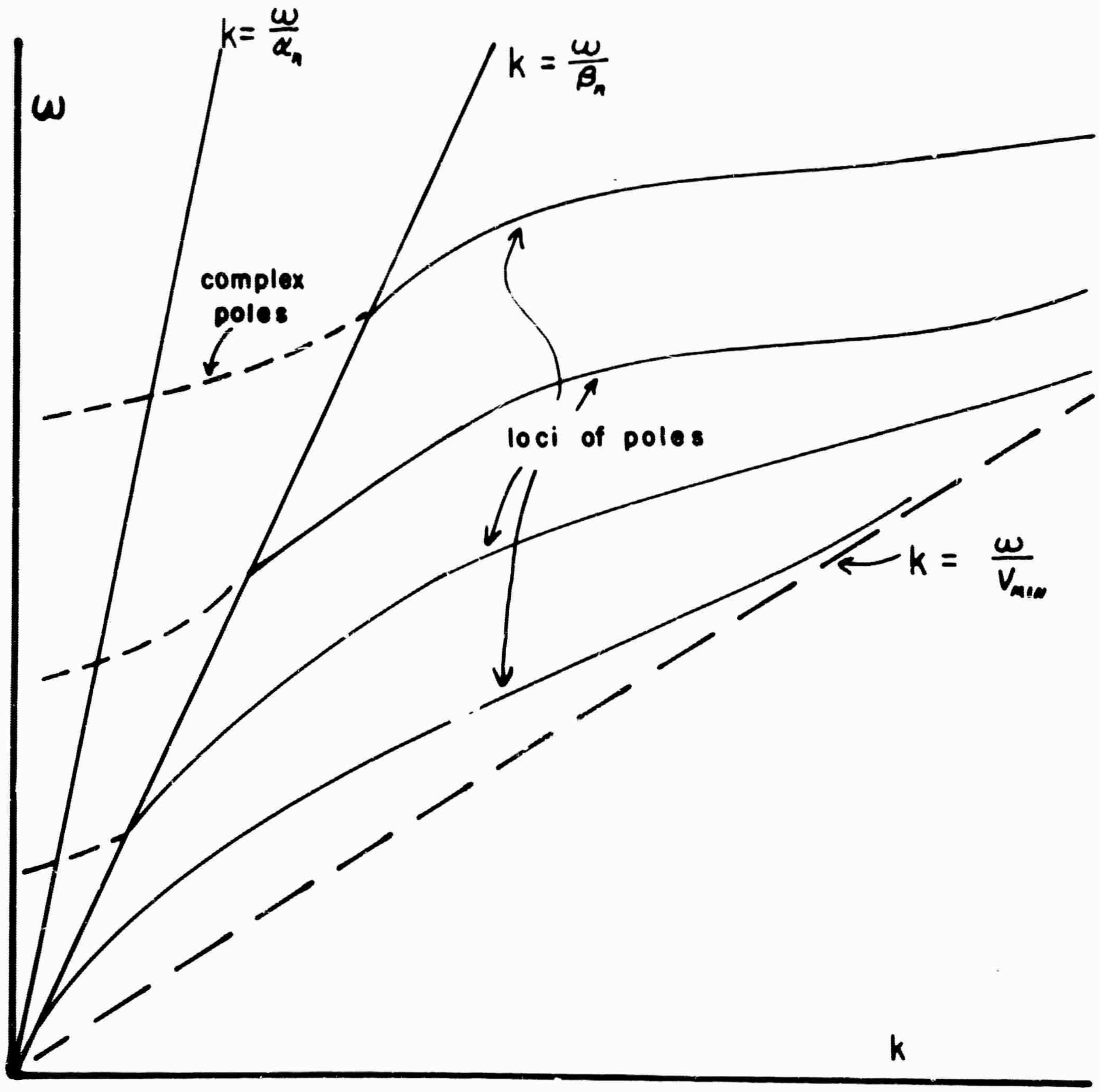

$k = \frac{\omega}{\alpha_n}$
$k = \frac{\omega}{\beta_n}$
ω
complex poles
loci of poles
$k = \frac{\omega}{V_{min}}$
k

Figure 2

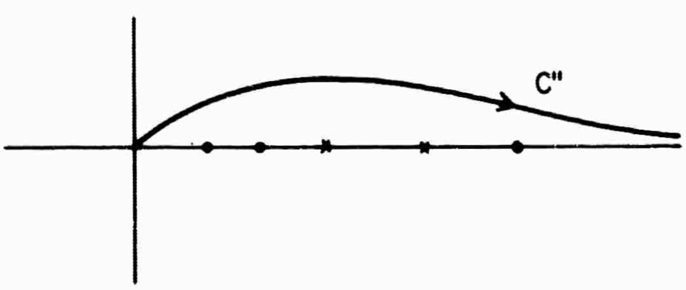

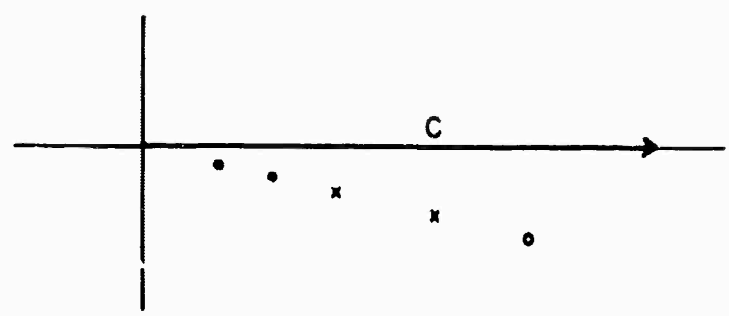

Figures 3a and 3b

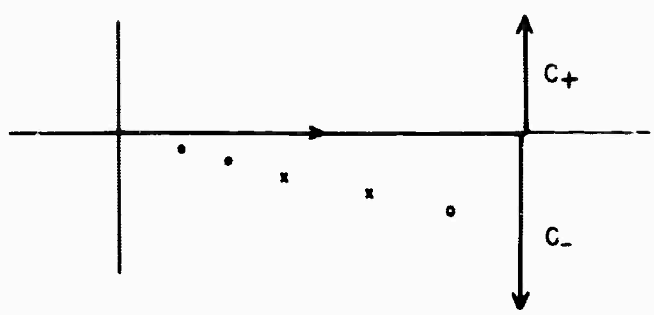

Figure 4

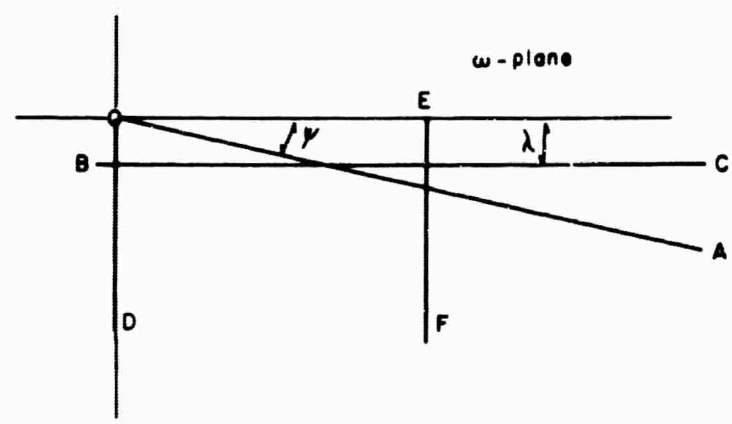

Figure 5

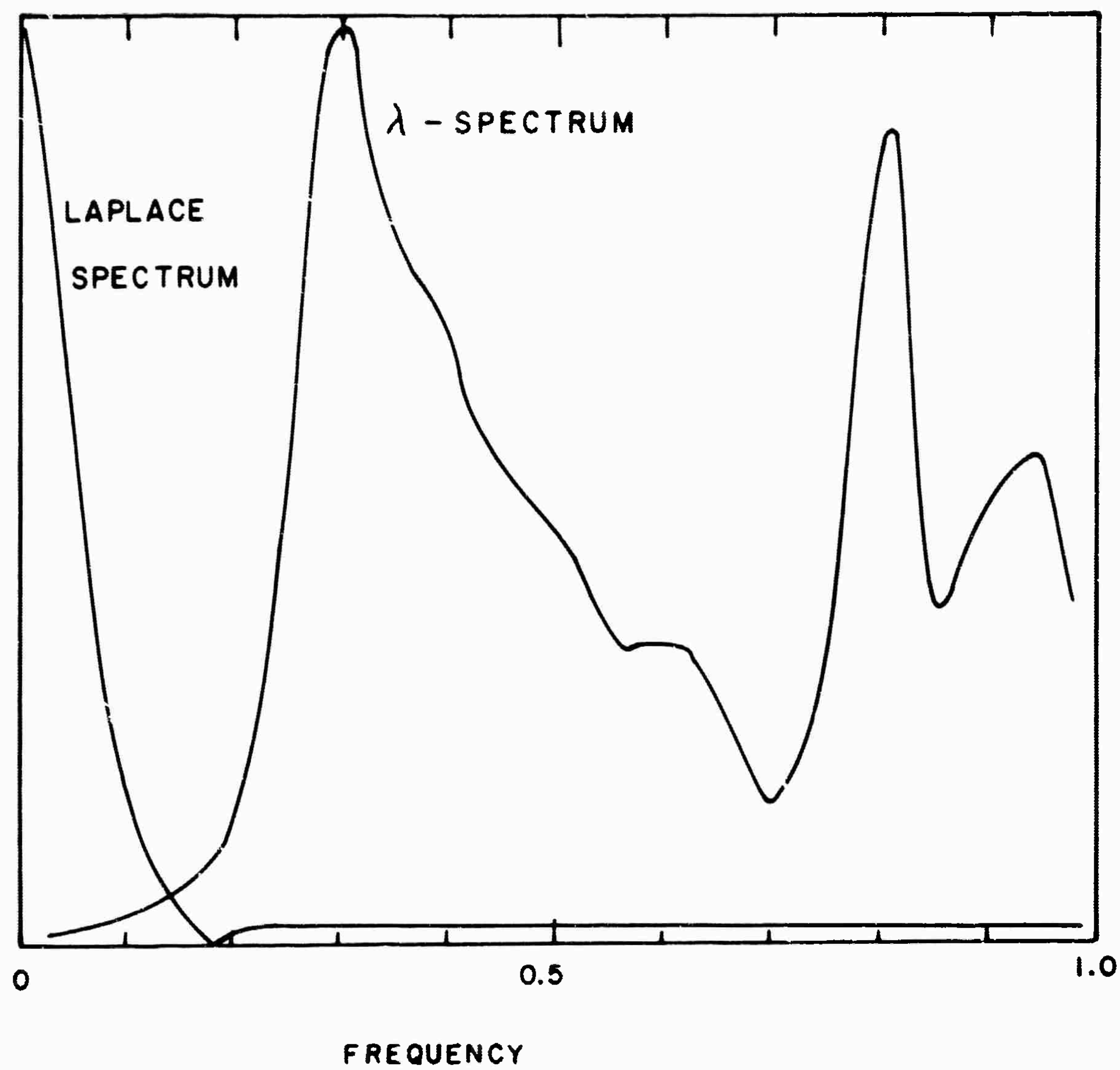

Figure 6

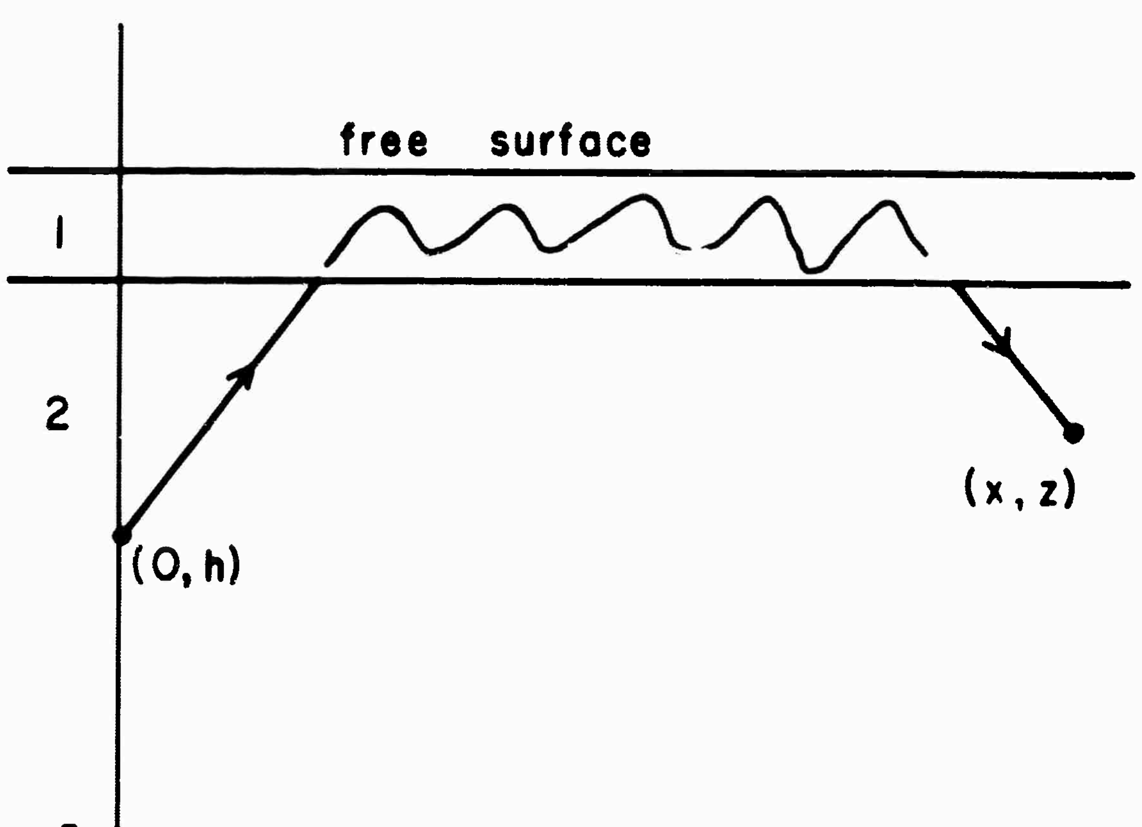

Figure 7

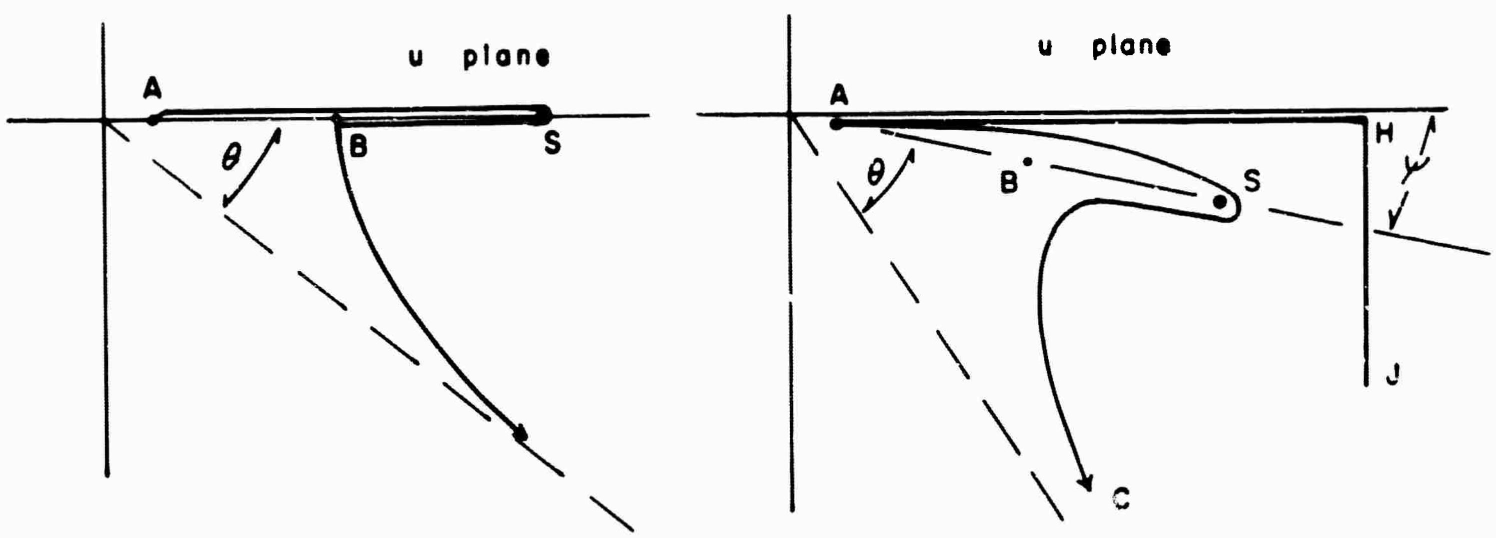

Figures 8a and 8b

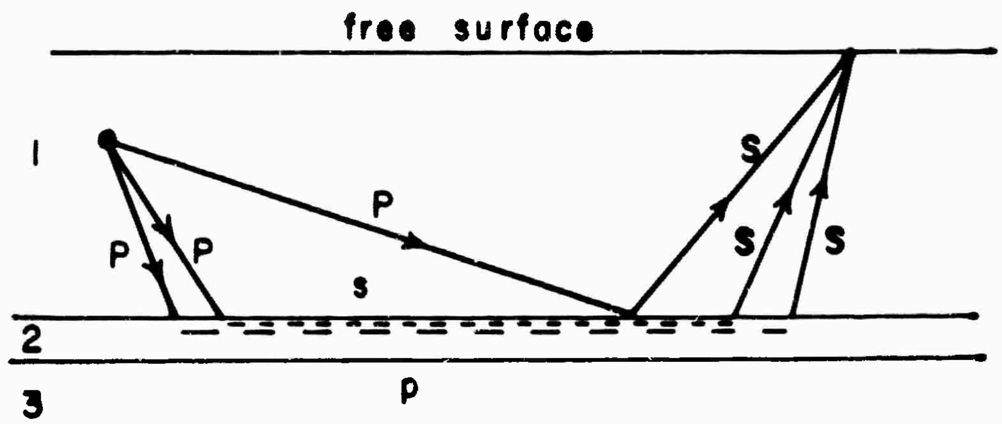

Figure 9

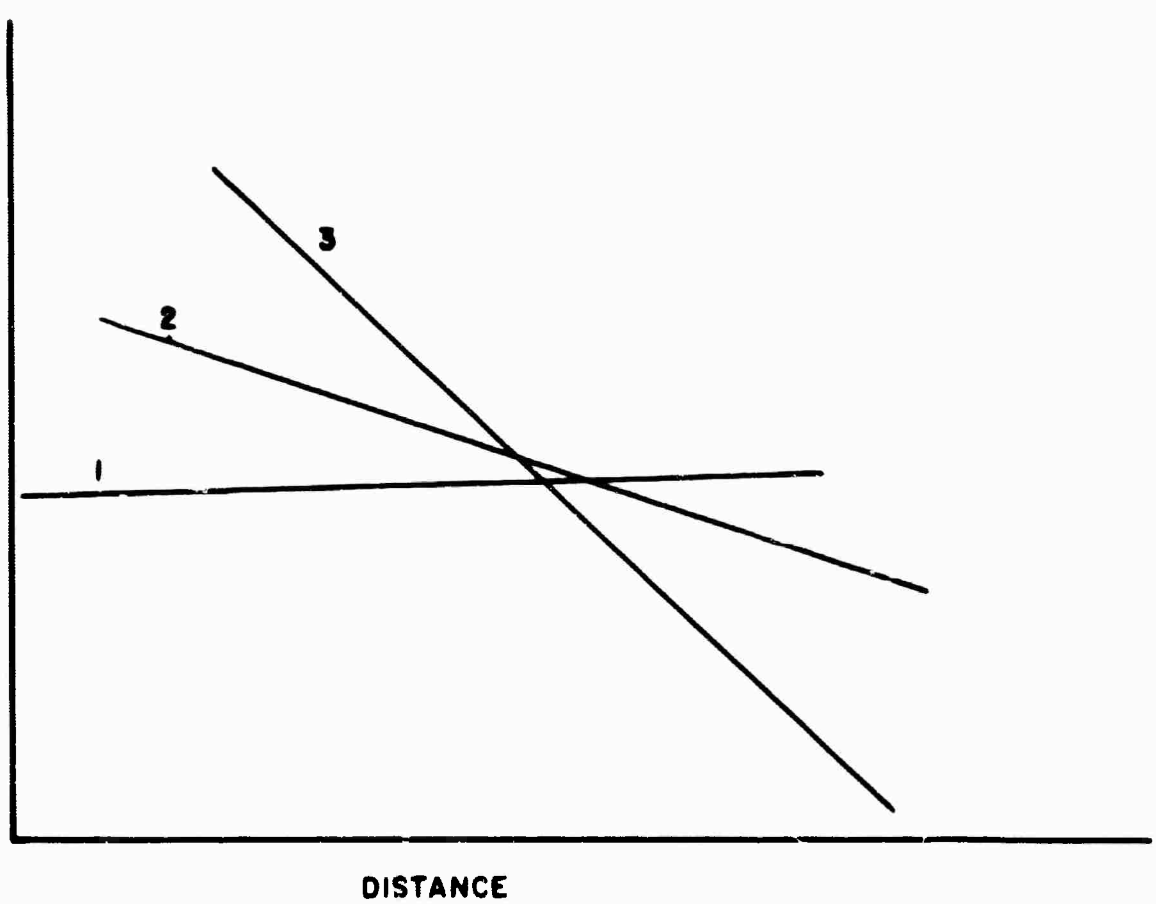

Figure 10

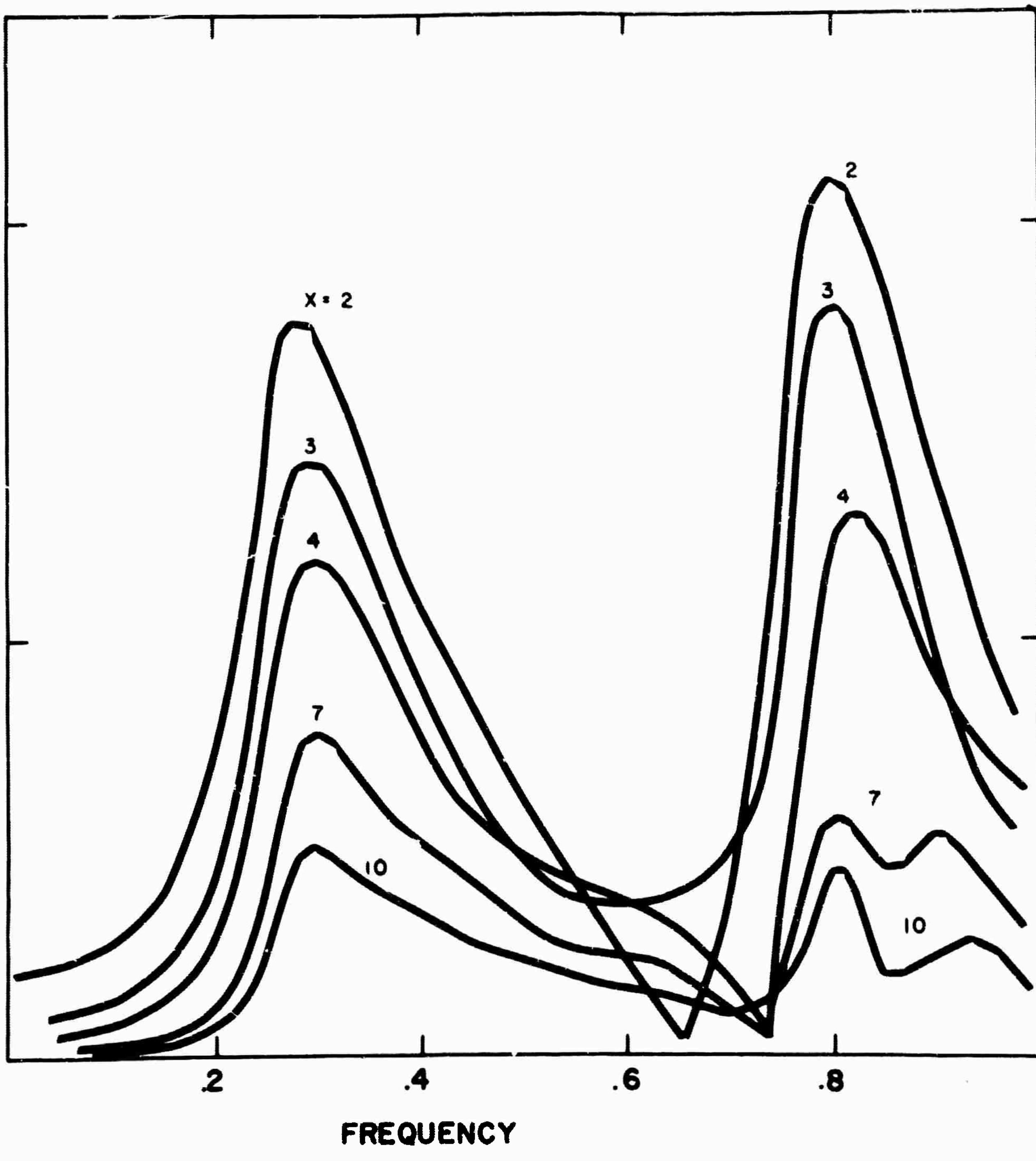

Figure 11

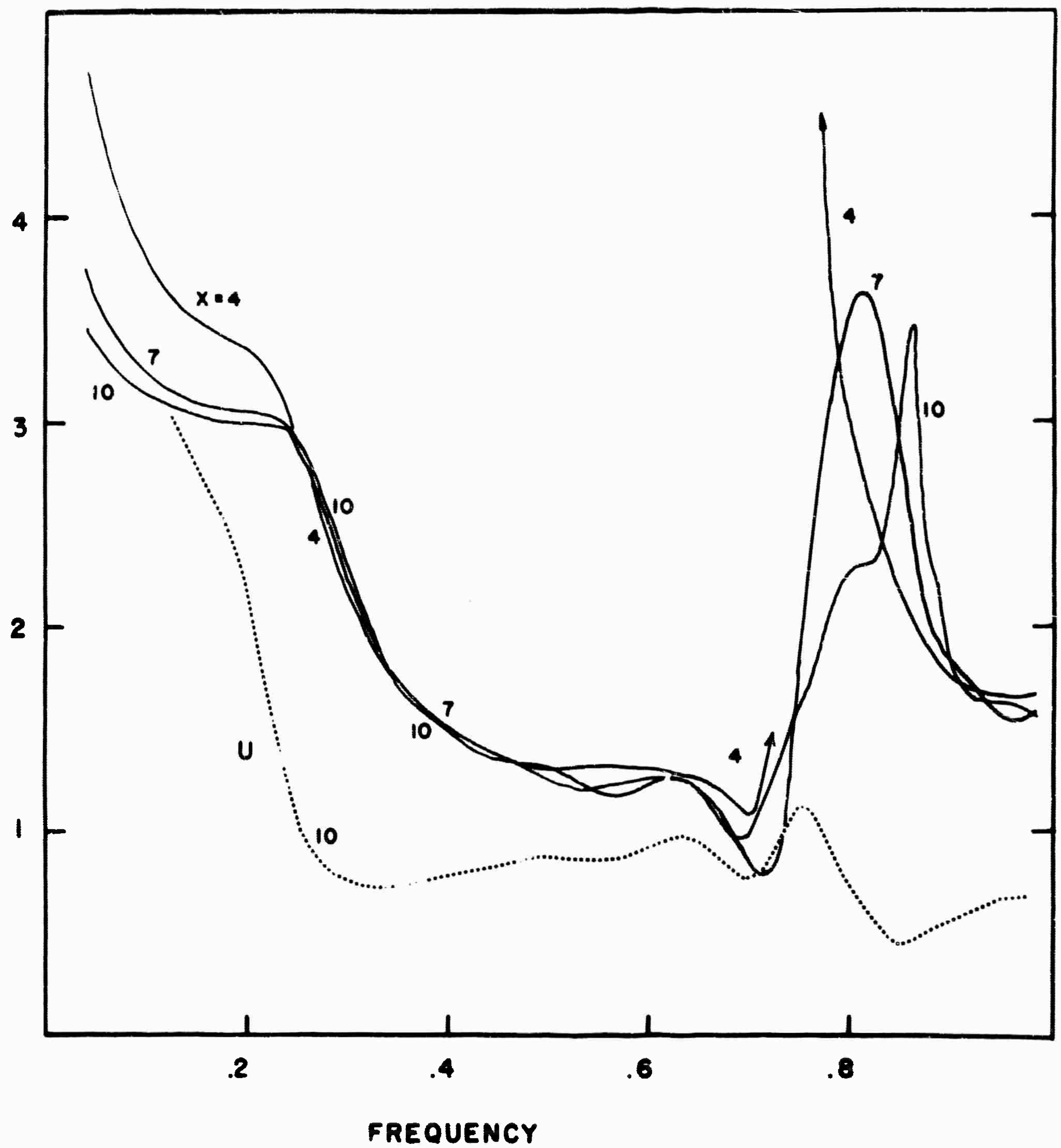

Figure 12

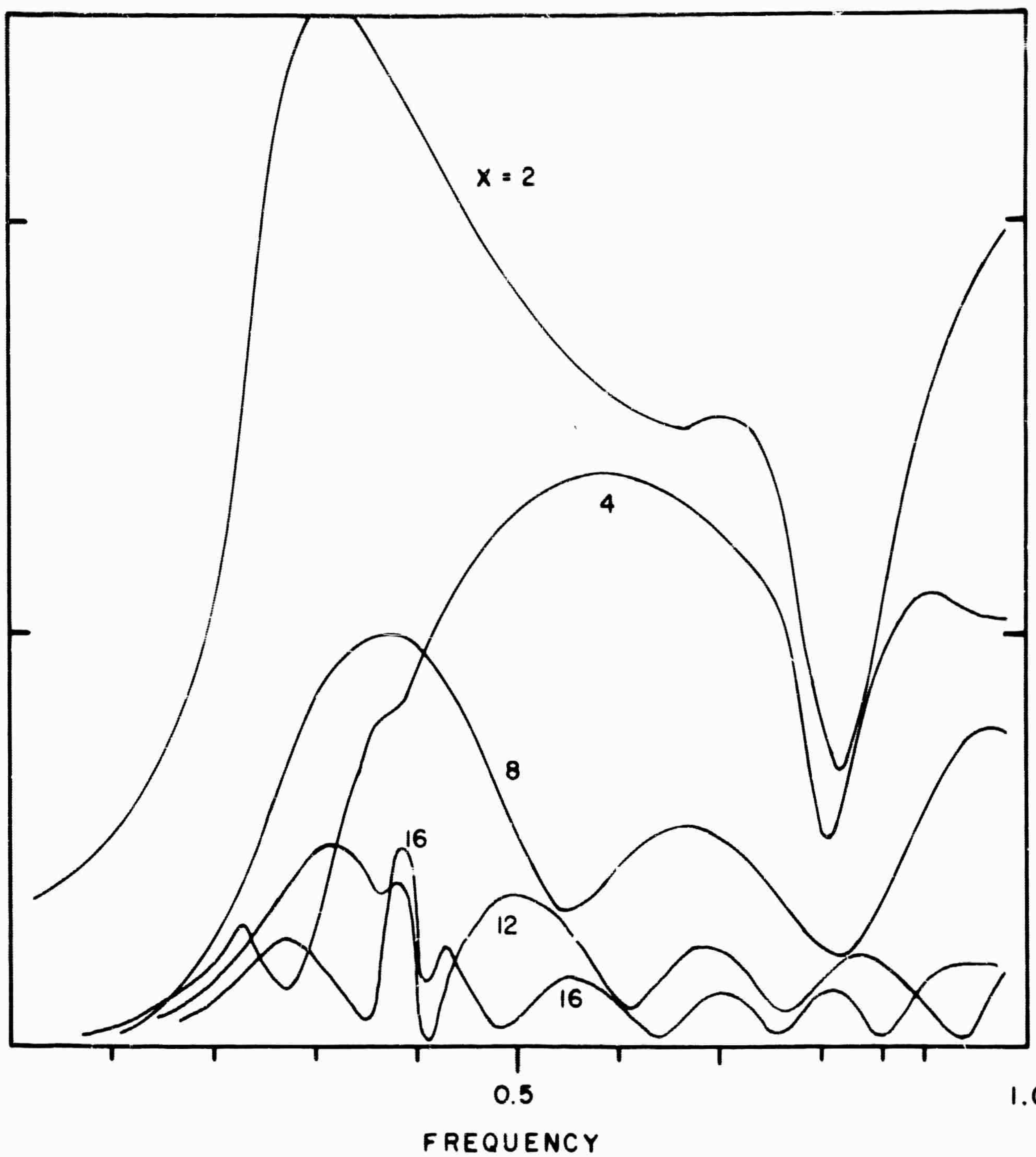

Figure 13

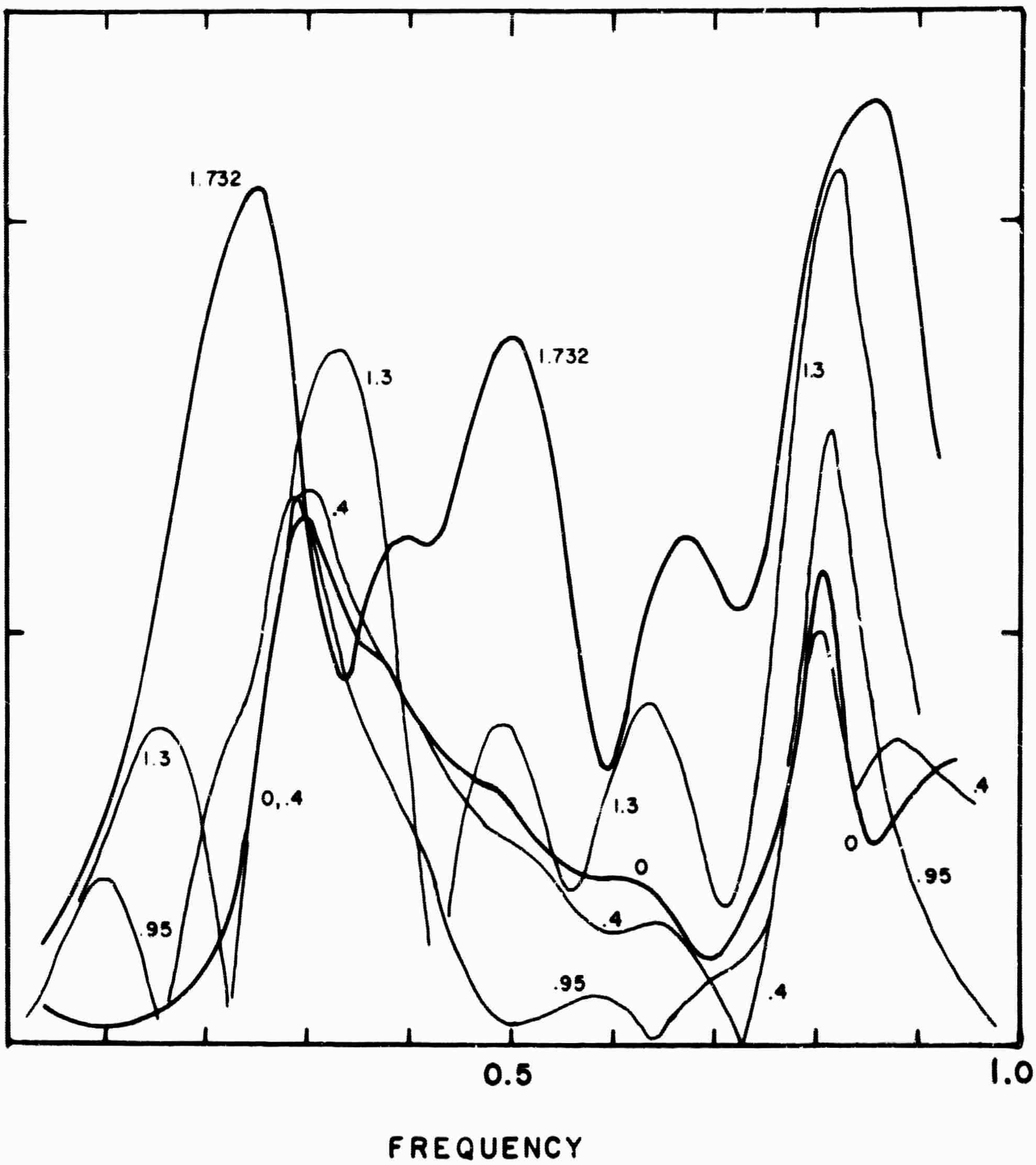

Figure 14

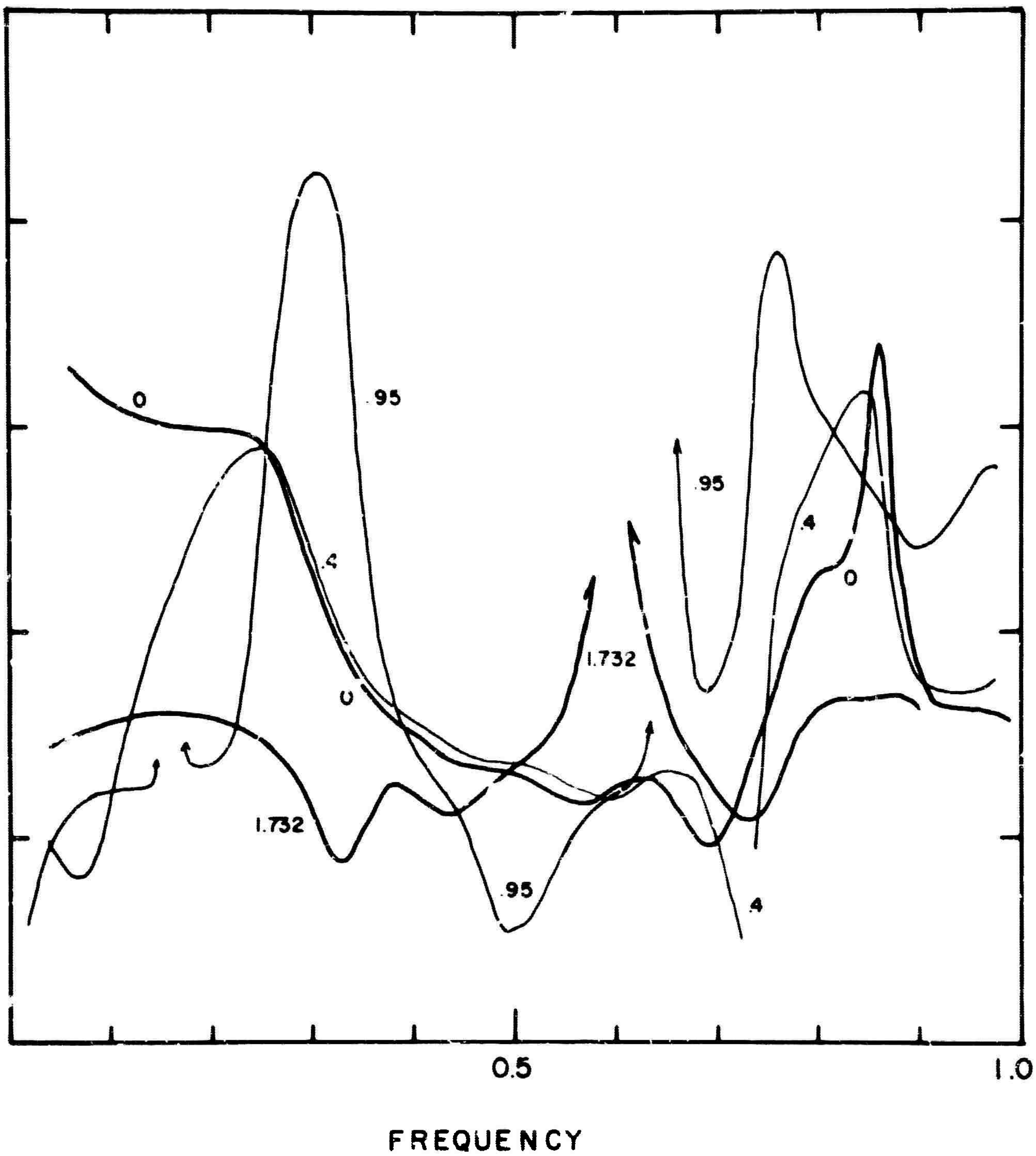

Figure 15

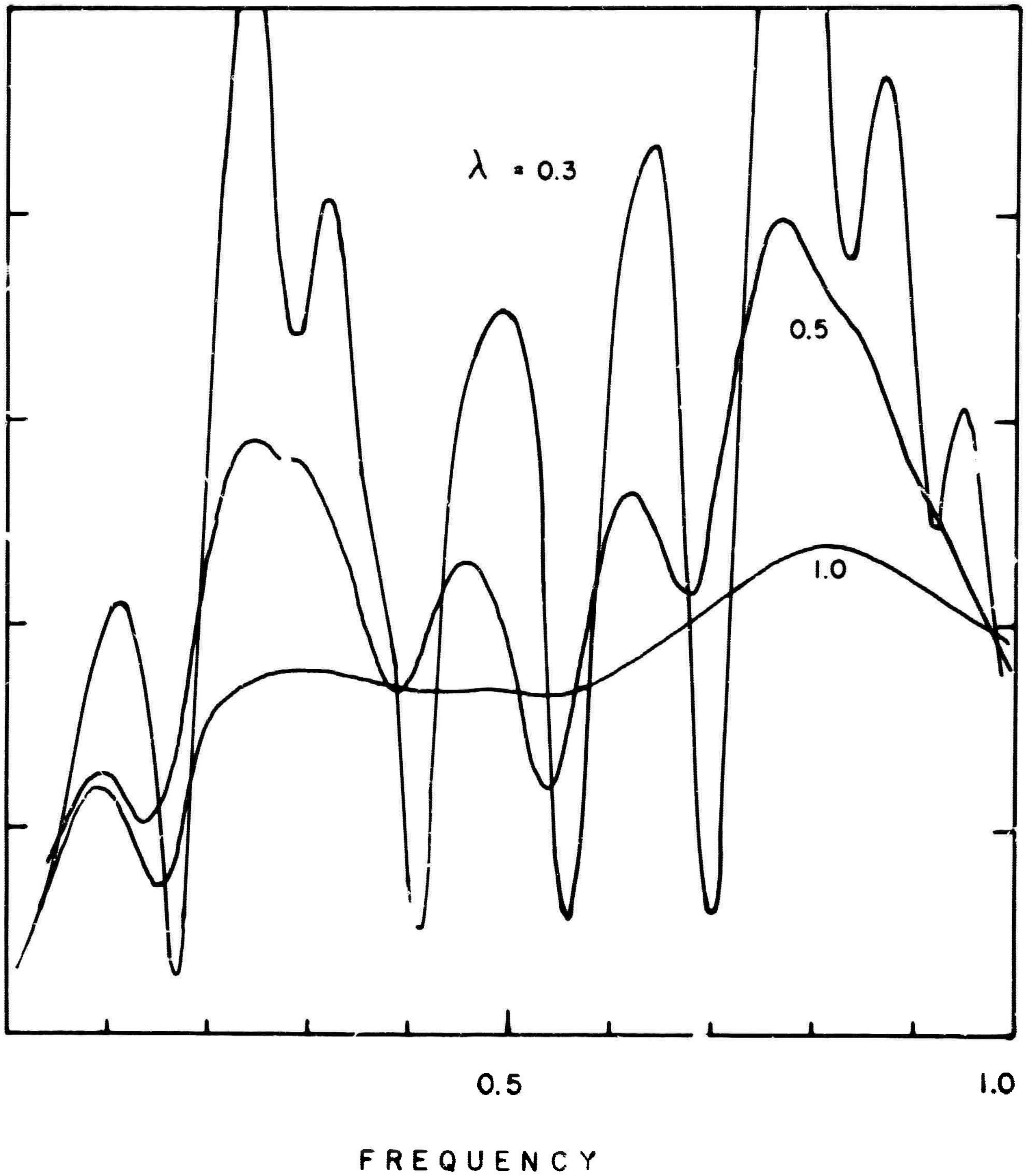

Figure 16

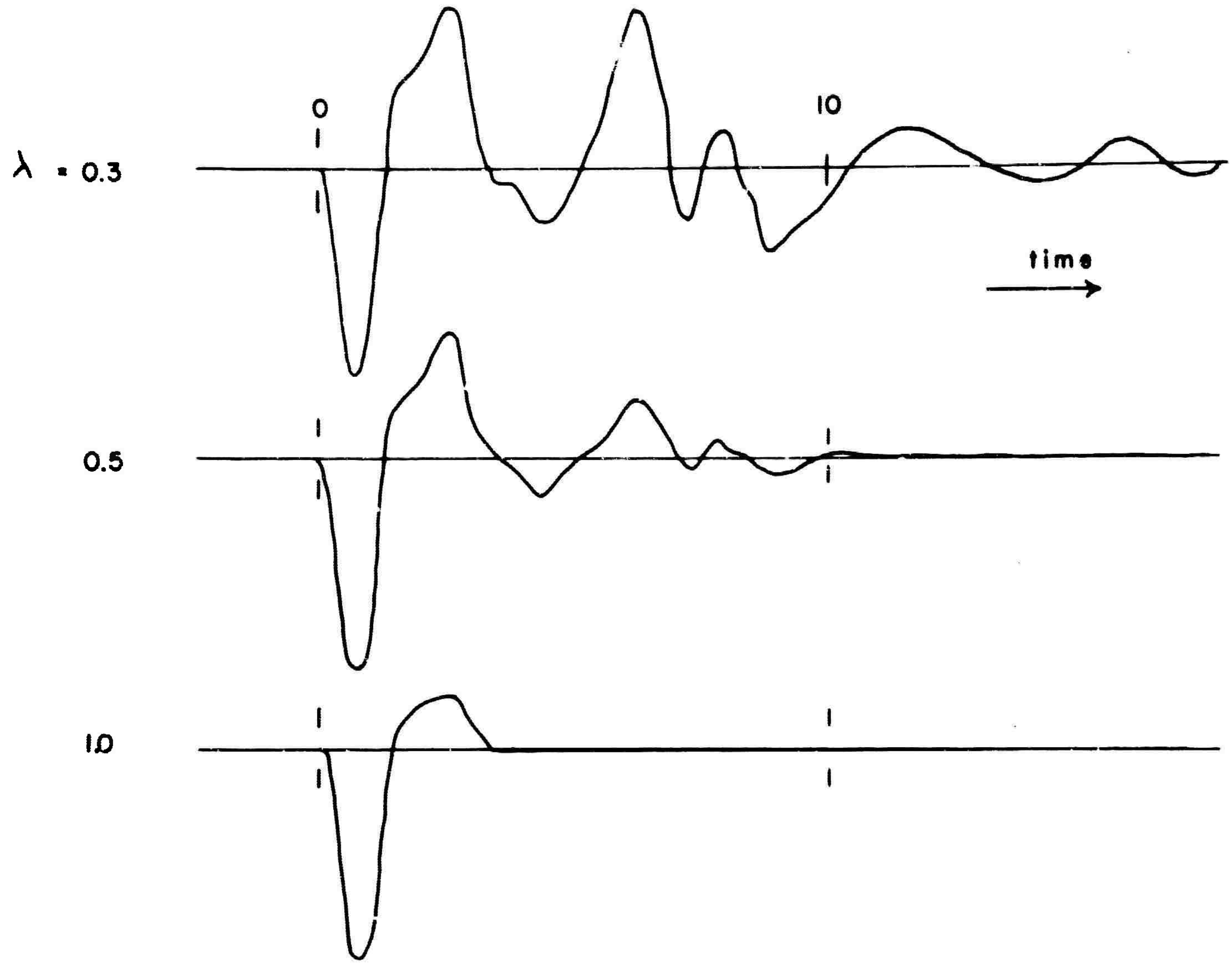

Figure 17